Check for updates

TRR
JOURNAL OF THE TRANSPORTATION RESEARCH BOARD

Research Article

Transportation Research Record
1–19
© The Author(s) 2026
Article reuse guidelines:
sagepub.com/journals-permissions
DOI: 10.1177/03611981261448530
journals.sagepub.com/home/trr
Sage

Quantifying Self-Explaining Road Performance in Spiral Tunnels: Semantic-Based Evaluation and Simulation Validation

Yanzi Xia[1], Chi Zhang[1], Bo Wang[1], Xiaomin Yan[1], YanYang Gao[1], Yijing Zhao[2], and Min Zhang[2]

Abstract

In spiral tunnels, high cognitive load and elevated operational risks are prevalent because of visual monotony and geometric ambiguity. This study develops a quantitative model of the self-explaining level based on the "self-explaining roads" theory, integrating environmental semantic segmentation and a three-level situational awareness model. The model introduces perceptual and comprehension attribute indicators and is validated through driving simulation experiments involving 27 participants across six spiral tunnel scenarios. The results indicate that the proposed model effectively reflects the self-explaining level of roads, with a correlation coefficient with behavioral indicators ranging from −0.234 to −0.326, indicating smoother driving behavior as the self-explaining level increases. As the curve radius increases, the self-explaining level also increases (e.g., 9.9 at radius [R] = 250 m, 21.0 at R = 500 m, 27.6 at R = 970 m). The performance in right-turn scenarios is better than that in left-turn scenarios (20.0 for right turns and 19.0 for left turns). The simulation adopted a left-side driving configuration, consistent with the design assumption for passenger vehicles in the studied tunnel scenario. In this study, drivers were guided to drive in the right lane. Additionally, entrance and exit areas introduce cognitive fluctuations because of abrupt changes in lighting and structure, highlighting the need for targeted optimization in these critical zones. This research provides a quantitative tool and methodological foundation for evaluating the safety of spiral tunnels, paving the way for future exploration into optimized design strategies and underlying cognitive mechanisms.

Keywords

self-explaining roads, spiral tunnels, driving cognition, semantic segmentation, situational awareness

Introduction

Mountain roads are characterized by complex terrain and significant elevation differences, making construction highly challenging. As a typical structure used to overcome elevation changes, spiral tunnels have been widely adopted in highway construction because of their ability to achieve spatial transitions through continuous unidirectional curves (*1*–*3*). These tunnels are generally composed of successive curves in the same direction, featuring long lengths and large curvatures. While such geometric characteristics help adapt to the mountainous terrain, they also lead to visual monotony and induce psychological rotation effects, which can increase drivers' cognitive load and elevate the risk of operational deviations and safety hazards (*4*, *5*). From a safety perspective, the abrupt variation in geometric design parameters (e.g., lane width, curvature, gradient) at spiral tunnel entrances, coupled with sustained curvilinear alignment, can induce driver misinterpretation of operational demands. Therefore, it is necessary to understand the impact of the geometry and environment of spiral

[1]School of Highway, Chang'an University, Xi'an, Shaanxi, China
[2]School of Transportation Engineering, Chang'an University, Xi'an, Shaanxi, China

Corresponding Author:
Chi Zhang, zhangchi@chd.edu.cn

tunnels on driving performance from the perspective of driver perception and behavioral response.

The "self-explaining roads" (SER) theory provides an effective approach to addressing such cognitive challenges. Proposed by Theeuwes and Godthelp, the core of this theory lies in promoting consistency between driver cognition and road environment design, enabling drivers to "read" the road and make the "right responses" (*6*). In recent years, the SER theory has been widely applied to tunnel studies, particularly in evaluating the performance of localized elements such as visual guidance facilities, signage, and pavement color, yielding significant progress and offering empirical support for their safety benefits (*7–9*). Related studies have employed methods including questionnaires, perception experiments, and driving simulations to systematically assess how various facilities influence driving behavior. Some researchers have further incorporated subjective speed perception, gaze behavior, curvature illusion, and situational awareness models to reveal the cognitive mechanisms and effectiveness of SER-based interventions in tunnel environments from multiple dimensions (*7–11*). For example, Jiao et al. systematically evaluated the self-explanatory performance of various visual guidance facilities in urban tunnels through speed perception experiments based on subjective speed equivalent sensing and perceptual reaction time (*8*). Theeuwes et al. quantitatively assessed the impact of different road elements on drivers' speed selection through large-scale questionnaire experiments using static road images as stimuli (*12*). Xia et al. quantitatively identified the effects of key environmental elements on drivers' gaze behavior and curvature illusion in spiral tunnels through questionnaire surveys and curvature perception experiments (*13*). Yan et al. and Xing et al. evaluated the self-explanatory performance of SER facilities based on driving simulation experiments, using behavioral and eye movement indicators such as spatial perception, visual attention, lane deviation, following distance, and steering stability (*7*, *9*). In addition, Yan et al. incorporated the three-level situational awareness model in their quantification, revealing drivers' understanding and response mechanisms to tunnel environments (*9*, *11*).

However, most current research focuses on performance evaluation, and there is still a lack of quantitative understanding of the theoretical processes and human-environment interaction mechanisms behind these results. Driving cognition is influenced by the layout and activation level of visual information channels, which are, in turn, determined by the interaction between environmental salience and driving experience. These factors affect attention allocation and response speed (*14*, *15*). Relying solely on behavioral outcomes or single physiological indicators is insufficient to uncover these mechanisms. There is an urgent need to investigate the full process by which environmental elements are perceived, understood, and transformed into behavior during dynamic driving (*16*, *17*).

Against this backdrop, image semantic segmentation offers a new approach to analyzing the mechanisms by which various environmental elements contribute to road self-explanation. In the U.S., research on self-enforcing roads has explored image recognition and data modeling frameworks, emphasizing the role of environmental design in encouraging drivers to intuitively regulate speed to enhance safety (*18*). Building on this, Ren et al. developed a semantic segmentation and visual sensitivity model to quantitatively assess the impact of rural road elements on driving behavior, and evaluated their guidance effectiveness based on SER theory (*19*). To date, numerous studies have examined the semantic components of tunnel environments that influence driving behavior, including road curvature, visual guidance devices, traffic signs, tunnel walls, and transition zones (*20–29*). These findings provide a valuable reference for the semantic classification used in this study.

Although numerous studies have improved the interpretability of tunnel environments, challenges remain when addressing complex structures such as spiral tunnels, which are characterized by continuous spatial variation. A critical gap in existing spiral tunnel studies is the lack of focus on safety hazards induced by mismatches between cognitive processing and geometric design. Key limitations include the lack of a quantifiable model linking driver cognition with environmental elements, unclear alignment between environmental design and specific driving conditions, and an insufficient understanding of the relationship between cognitive precursors and behavioral adaptation. Therefore, it is essential to translate the concept of SER into an application-oriented framework with practical engineering value. In addition, turn direction was also considered, as left- and right-turn spiral tunnels may impose different perceptual and control demands on drivers. The simulation adopted a left-side driving configuration, consistent with the design assumption for passenger vehicles in the studied tunnel scenario. In this study, drivers were guided to drive in the right lane. To this end, this study proposes an assessment method for evaluating the self-explaining level of spiral tunnels, which includes: 1) developing a quantification model based on semantic segmentation, 2) validating the feasibility of the model, and 3) analyzing the influence of key spiral tunnel characteristics on SER performance. The proposed evaluation framework provides a quantitative tool for assessing the self-explaining level of spiral tunnel and can support the design and optimization of tunnel facilities aimed at enhancing driver cognitive performance.

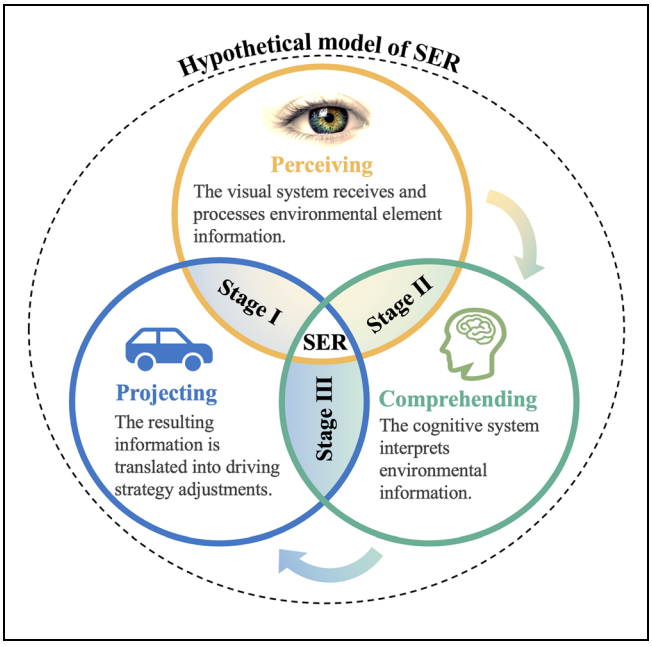

Figure 1. Hypothetical model of self-explaining roads (SER).

Figure 2. Features extracted via semantic segmentation.

Methods

Hypothetical Model of SER

Previous SER approaches have referenced various cognitive precursors to explain ideal behavioral adaptation; however, the use of situational awareness theory offers a unified framework for these concepts (*30*). Assuming the driver acts as a Bayesian observer, and building on the SER hypothesis model proposed by Theeuwes—which suggests that roads should be quickly and easily perceived and understood by drivers to facilitate correct decision-making—this study integrates attention resource theory to establish a set of indicators (*31*, *32*). This framework comprehensively captures the entire process from environmental information input to driving behavior output, as illustrated in Figure 1.

Extraction of Environmental Features Based on Semantic Segmentation

According to SER theory, a driver's selection of environmental information results from the interaction between their driving goals and the visual attributes of the environment. To quantify this process, this study employs semantic segmentation to extract the semantic composition of tunnel scenes. Compared with other visual models, Mask2Former aligns more closely with the human visual mechanism of "local attention–global integration" (*33*, *34*). Therefore, it is selected to achieve high-precision panoptic segmentation, outputting semantic labels, masks, and multi-scale dimensional information, as illustrated in Figure 2. A state-of-the-art model—"mask2-former_swin-t_8xb2-90k_cityscapes"—was adopted (*35*). Based on the characteristics of drivers' visual search behavior and relevant classification standards, the tunnel environment semantics are categorized into four classes: visual guidance facilities, traffic signs, the overall environment, and the roadway region (*19*).

Evaluation Model of Self-Explaining Level

Specifically, according to the situation awareness model, the process of driving assignment typically goes through three stages: perception, comprehension, and action (as shown in Figure 3). In the perception stage (Figure 3*a*), environmental salience and saccade amplitude reflect the driver's visual extraction efficiency of road information. Higher environmental salience and moderate saccade amplitude help reduce cognitive load and improve perception speed. In the comprehension stage (Figure 3*b*), fixation duration and LH/FH ratio reflect the cognitive consumption of the driver during information processing. Longer fixation duration and a higher LH/FH (Low-Frequency/High-Frequency) ratio indicate higher cognitive load. In the action stage (Figure 3c), the level of self-explanation is manifested through the driver's behavioral feedback (i.e., speed control and trajectory control). Therefore, a higher self-explaining level is usually accompanied by the smoothness and stability of driving behavior.

Perceptual Attribute of the Road: f_{ij}. During the perception phase, environmental information is received and processed by the driver's visual system. To quantify its visual attributes, this study adopts a saliency metric A_{ij} based on attention resource theory to represent the visual prominence of environmental elements (Equation 1).

$$A_{ij} = a_{(i+1)j} \times n_{(i+1)j} \quad (1)$$

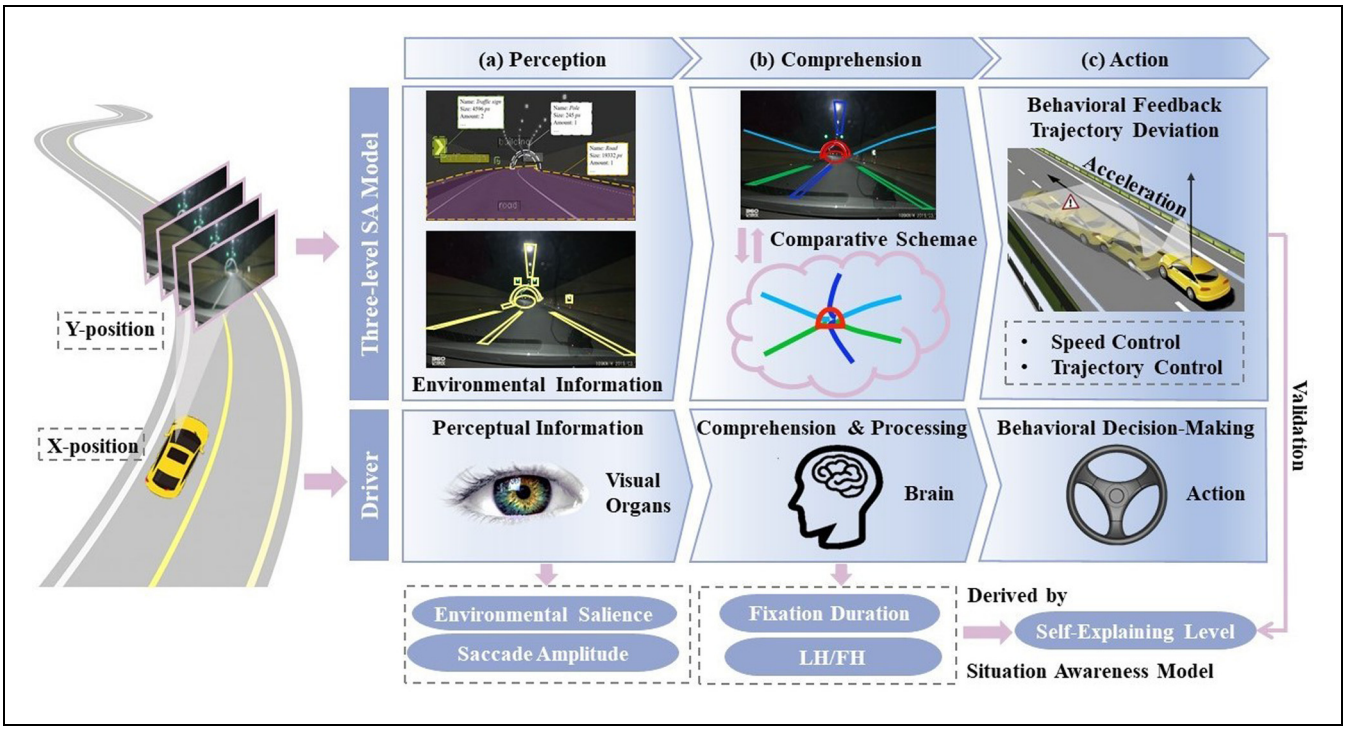

Figure 3. Overview of the self-explaining level evaluation model, illustrating the three stages of the driver's road perception process.
Note: LH/FH = Low-Frequency/High-Frequency; SA = Situation Awareness.

where
i = the driving unit (the saliency is derived from the image at the location of the subsequent driving unit),
j = one of the four semantic categories,
a_j = the area (in pixels) within category j, and
n_j = the number of elements within category j.
The metric A_{ij} reflects the objective salience of environmental semantic category j perceived by the driver at position i.

Considering the randomness and fuzziness in human information processing, this study draws on a variant of Shannon entropy from fuzzy entropy theory to model the importance membership degree $u_j \in [0, 1]$, $j = 1, 2, 3, 4$ of input information (*14*). Through exponential transformation and normalization, the importance weights U_j for each semantic category are derived to represent the subjective influence of the driver's experience and preferences on the salience of that category. Therefore, this parameter is obtained from the driver's subjective ratings of the four semantic categories. The environmental semantic saliency of the entire scene can be obtained through calculation using Equation 2. A_j, by integrating the objective salience of the information and the driver's subjective preference, represents the salience of the j-th category of environmental semantics; a larger A_j indicates that this semantic category is more prominent and can be more readily perceived by the driver.

$$A_j = U_j \times \sum_{1}^{i} A_{ij} \tag{2}$$

According to attention resource theory, cognitive effort can be quantified by the attentional cost associated with shifting focus across different perceptual regions, which is commonly measured by saccade distance (*14*, *36*). In this study, the effort E_i a driver expends to acquire environmental information is represented by saccade amplitude. To reduce inter-individual differences, the raw saccade amplitude was normalized for each participant using that participant's overall mean value across all scenarios and analysis units. Therefore, E_i denotes a dimensionless relative saccade amplitude. By integrating the saliency metric, the perceptual attribute of the road is calculated using Equation 3. A larger f_{ij} indicates that the driver can acquire highly salient environmental information with a lower attentional shifting cost, implying higher information acquisition efficiency in that region.

$$f_{ij} = \frac{A_j}{E_i} \tag{3}$$

Comprehensive Attribute of the Road: V_i. According to the theory of SER, road environments should be easy for drivers to comprehend, thereby minimizing the consumption of cognitive resources. Based on attention resource theory and the energy-efficient decision-making model, the cognitive resources consumed by a driver can be expressed as the product of cognitive activation level and the subjective importance of information (*14*, *37*). In this context, the cognitive activation level δ_i is assessed using the LF/FH ratio derived from heart rate variability, while the subjective importance is reflected by the fixation time t_i on key regions of interest (*9*). To reduce inter-individual differences in physiological and visual-response baselines, both the LH/FH ratio and fixation time were normalized for each participant using that participant's mean value across all scenarios and analysis units. The comprehension attribute V_i of the road is then constructed as the reciprocal of this product, using Equation 4.

$$V_i = (\delta_i \times t_i)^{-1} \tag{4}$$

Road Self-Explaining Level: S_i. According to the three-level situational awareness model, drivers process road information in a top-down hierarchy consisting of perception, comprehension, and projection, each occurring with certain probabilities (*11*). In this study, three events are defined:

- a_i: successful perception
- b_i: successful comprehension
- c_i: successful projection

The probabilities of these events are calculated by Equation 5:

$$P(a_i) = \frac{f_i^*}{\sum f_i^*}, P(b_i|a_i) = \frac{V_i}{\sum V_i}, P(c_i|a_i b_i) = 0.53 \tag{5}$$

where

f_i^* = the sum of all scenario values.

Correspondingly, driving cognition is divided into four states, each associated with a cognitive level $L_k = 0, 0.4\,0.8, 1$ (*38*). The final self-explaining level is expressed as a mathematical expectation, which comprehensively reflects the degree of cognitive completion across the three SA (Situation Awareness) stages. The formulation is presented in Equation 6:

$$\begin{aligned} S_i = \sum_{k=1}^{n} P(a_i, b_i, c_i) \times L_k = P(\overline{a}_i) \times 0 + P\left(a_i \overline{b}_i\right) \\ \times 0.4 + P(a_i b_i \overline{c}_i) \times 0.8 + P(a_i b_i c_i) \times 1 \end{aligned} \tag{6}$$

Statistical Analysis

To provide behavioral validation of the proposed model, the association between the self-explaining level S_i and two driving performance indicators, namely acceleration and trajectory deviation, was examined using Spearman's rank correlation analysis. This nonparametric method was adopted because it aims to assess the monotonic relationships without assuming normality of variables. Correlation analyses were conducted separately for each scenario. To control the family-wise error rate arising from multiple comparisons, Bonferroni correction was applied, and the adjusted significance threshold was set at $p' < 0.05/n$, where n denotes the total number of statistical comparisons performed in the analysis. All reported p-values were two-sided.

Experiment

Design of Scenes

This study employs a driving simulation experiment to validate the proposed model. The experiment design includes six typical scenarios, as shown in Figure 4. The simulation scenes were constructed using UC-win/Road (v8.1.2), based on a spiral tunnel located in western China. The total central angle was set to 330°, a full circular horizontal curve with a 155° central angle was adopted for the spiral tunnel, and a constant longitudinal grade of 2.8% was applied throughout the tunnel segment (uphill for left-turn scenarios). The simulation adopted a left-side driving configuration, consistent with the design assumption for passenger vehicles in the studied tunnel scenario. No surrounding traffic vehicles were included in the simulation environment, to isolate the influence of road environmental features on driver perception.

More specifically, the road cross-section adopted a unidirectional two-lane configuration, with each lane having a width of 3.75 m; the road cross-section remains consistent along the entire tunnel. Facility parameters of the simulated tunnel are shown in Table 1. All facility designs were developed in accordance with the Chinese specifications for tunnel traffic safety facilities. The unit definition and spacing calculation method for retroreflective rings followed Du et al. (*39*).

Platform and Participants

The experiment was conducted using a high-fidelity, multi-degree-of-freedom driving simulator. The experiment setup and equipment are shown in Figure 5. A total of 27 participants were recruited, with gender distribution aligned with the demographics of licensed drivers in China (*40*). All participants held valid driver's licenses

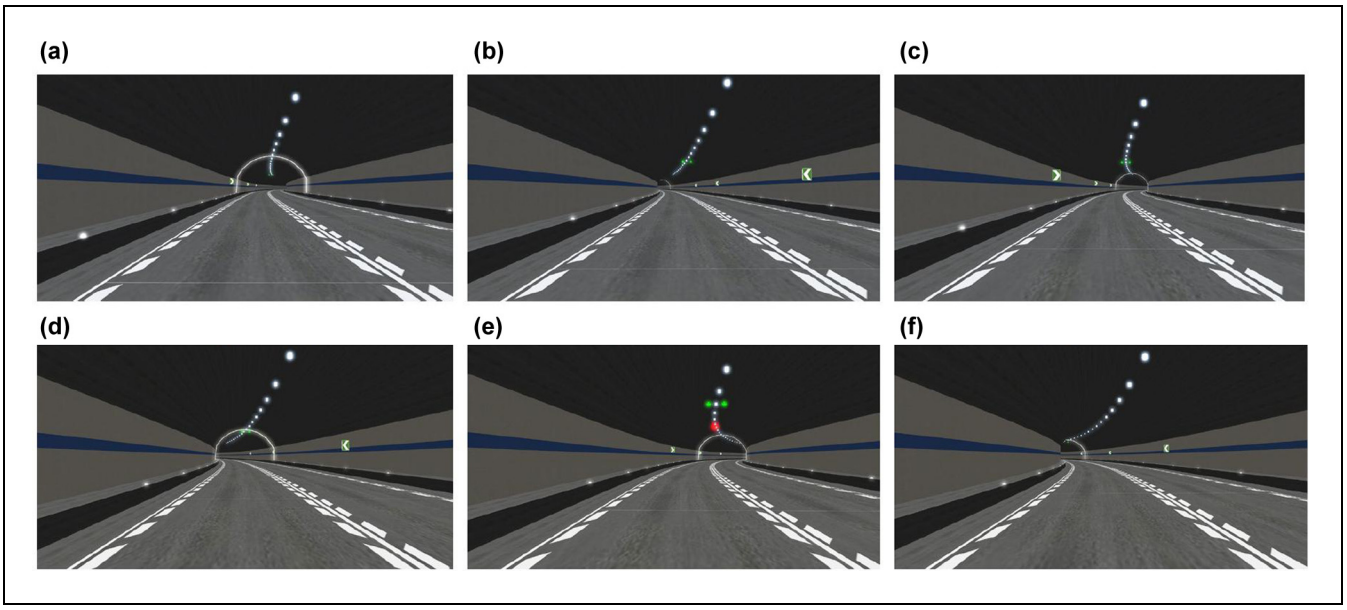

Figure 4. Modeled scene of spiral tunnels: (*a*) Scene 1, right-turn, R = 970 m, (*b*) Scene 2, left-turn, R = 970 m, (*c*) Scene 3, right-turn, R = 500 m, (*d*) Scene 4, left-turn, R = 500 m, (*e*) Scene 5, right-turn, R = 250 m, and (*f*) Scene 6, left-turn, R = 250 m.
Note: R = radius.

Table 1. Facility Parameters Used for Environmental Layout

Facility	Frequency or parameter
Retroreflective rings	1 visible
Edge markings	None
Chevron alignment signs	30 m spacing
Traffic signals	200 m spacing
Speed limit signs	200 m spacing
Lighting	White
Sidewall	Longitudinal blue bars
Lane separations	White solid lines

Note: Within 600 m of the tunnel entrance and exit, longitudinal deceleration markings were applied based on the real tunnel case in western China.

Figure 5. Experiment platform and facilities.

and had proficient driving experience. Data collection was carried out anonymously, and all participants received appropriate compensation for their involvement. The variables collected during the experiment are shown in Table 2.

Experiment Procedure

The experiment consisted of two phases: a preliminary test and the formal testing session, as detailed below.

1) In the preliminary test, participants were provided with detailed instructions about the driving simulator (e.g., how to start and brake). They were then asked to complete four sets of practice drives to become familiar with the simulated environment.
2) Before the formal experiment, the staff assisted the participants in wearing the eye tracker and wristband, and communicated with them to ensure that the devices had a negligible impact on driving behavior. Participants were also instructed to maintain a relatively stable head posture. Although minor head rotations may occur in natural driving, the experiment procedure aimed to minimize large head movements,

Table 2. Experiment Measurement Variables

Variable (unit)	Frequency	Index	Description of variable
Semantic size (px) and count	NA	$a_{(i+1)j}$, $n_{(i+1)j}$	Captured from images taken from the simulated road.
Significance of semantics	NA	u_j	Derived from participants' semantic rating scores.
Fixation duration (ms)	1,000 Hz	t_i	Directly exported from the software.
Saccade amplitude (px)	1,000 Hz	E_i	Directly exported from the software.
LH/FH	1,00 Hz	δ_i	Computed and exported by the software.
Acceleration ($m \cdot s^{-2}$)	10 Hz	NA	Directly exported from the software.
Trajectory deviation (m)	10 Hz	NA	Directly exported from the software.
Speed ($m \cdot s^{-1}$)	10 Hz	NA	Directly exported from the software.

Note: LH/FH = Low-Frequency/High-Frequency; NA = not available.

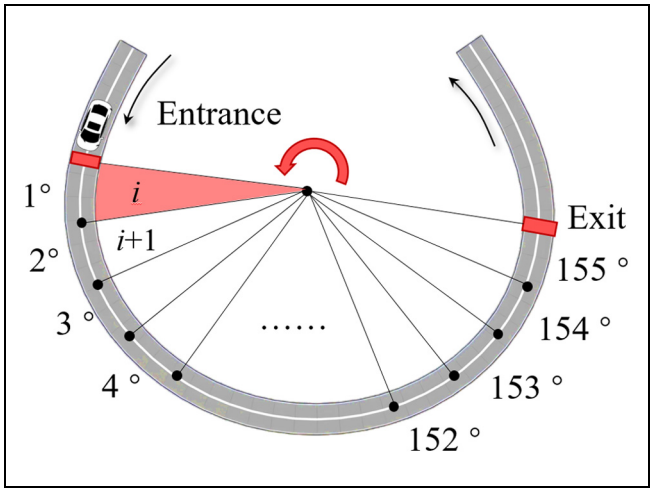

Figure 6. Cumulative turning angle as reference axis.

ensuring that most gaze shifts were captured by the eye-tracking system.

3) During the experiment, the participants were only informed that the speed limit inside the tunnel was 80 km/h. They were instructed to drive freely based on their individual driving habits and real-time responses to the simulated environment.
4) After each scenario, drivers were allowed to take sufficient rest. Notably, the order of the scenarios was randomized to eliminate order effects on the experiment results. Once a participant had completed all scenarios, the next participant was brought in, and the process was repeated until all participants had completed the driving simulation.

To maintain the integrity and reliability of the experiment data, staff were instructed to avoid interacting with participants during the experiment, ensuring a natural driving state. All devices were started and stopped simultaneously to minimize timing errors across data sources. The staff continuously monitored the data; if any anomalies were detected, the experiment was immediately halted.

To standardize data analysis across different scenarios, this study employed a time-series windowing method based on cumulative turning angle as a reference axis, avoiding information shifts caused by differences in travel time or distance. The total turning angle of the spiral tunnel was divided into equal intervals of 1 degree (Figure 6), and multi-source data were mapped to this dimension based on spatial and temporal alignment. The average value of observations within each window was calculated to reduce short-term fluctuations while preserving the overall behavioral trend. To minimize the risk that averaging over windows might obscure local changes, the angular step size was intentionally kept small, thereby maintaining sufficient temporal resolution. In addition, the variance of the parameters within each window was examined to verify that the averaging process did not mask the underlying trends.

It should be noted that for different tunnel radii, a fixed angular interval corresponds to different traveled distances. However, the use of cumulative turning angle as the reference axis allows behavioral data to be aligned with the geometric progression of the spiral tunnel. Although larger radii result in slightly longer spatial segments and potentially more observations within a window, all windows contained sufficient valid observations to ensure stable estimation of the averaged parameters.

Results

Correlation Analysis

Figure 7 presents the correlations between the self-explaining level S_i and the two objective driving performance indicators across the six spiral tunnel scenarios. In most tunnel scenarios, there was a significant correlation between the self-explaining level and driving behavior indicators. Especially in tunnels with larger (radius [R] = 970 m) and smaller (R = 250 m) curvatures, the correlation between the two is significantly negative

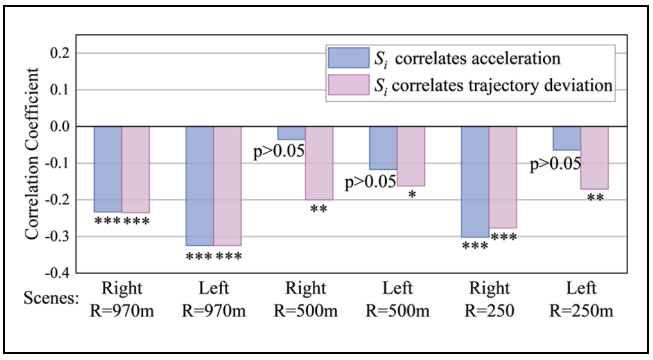

Figure 7. Correlation results between S_i values and objective driving performance indicators.
Note: After Bonferroni correction, * indicates $p<0.05$, ** indicates $p<0.01$, and *** indicates $p<0.001$; $p>0.05$ denotes no statistically significant correlation.

(correlation coefficients ranging from −0.234 to −0.326, with p-values all less than 0.001), indicating that the higher the self-explaining level, the smoother the driver's operation and the smaller the behavioral fluctuations. Especially in scenarios involving left-turn condition at R = 970 m and in the right-turn condition at R = 250 m, a statistically significant negative correlation is observed. In contrast, in tunnels with medium curvature (R = 500m), although the correlation with acceleration is weak (r = −0.036, p = 0.579), there is still a significant negative correlation between trajectory deviation and self-explaining level (r = −0.201, p = 0.00192). Overall, the results validate the effectiveness and applicability of the proposed model, demonstrating that the self-explaining level shows meaningful explanatory relevance for driving behavior.

Results of Perceptual Attribute of the Road

Visually Significance of Environmental Elements. The visual saliency calculation results for various environmental semantics under six working conditions are shown in Figure 8. For visual guidance facilities (A_1) (Figure 8 (*a*)), the numerical range is approximately 10.6–38.4, with the maximum (38.39) for right turn R = 970 m and the minimum (10.63) for right turn R = 500 m. The saliency values for left turn R = 970 m and left turn R = 250 m are 17.65 and 22.39, respectively. For medium radius R = 500 m, the saliency for left turn (13.69) is slightly higher than that for right turn. The saliency of traffic signs (A_2) (Figure 8 (*b*)), ranges from approximately 7.83 to 26.78, with the highest values (26.78 and 23.34) for right turn R = 970 m and right turn R = 250 m, respectively, while the values for both turns at R = 500 m are lower (7.83 and 9.91). The overall environment (A_3) (Figure 8 (*c*)), exhibits greater numerical differences, with the highest saliency (139.78) for right turn R = 250 m, followed by right turn R = 970 m (59.96), while the remaining conditions have values

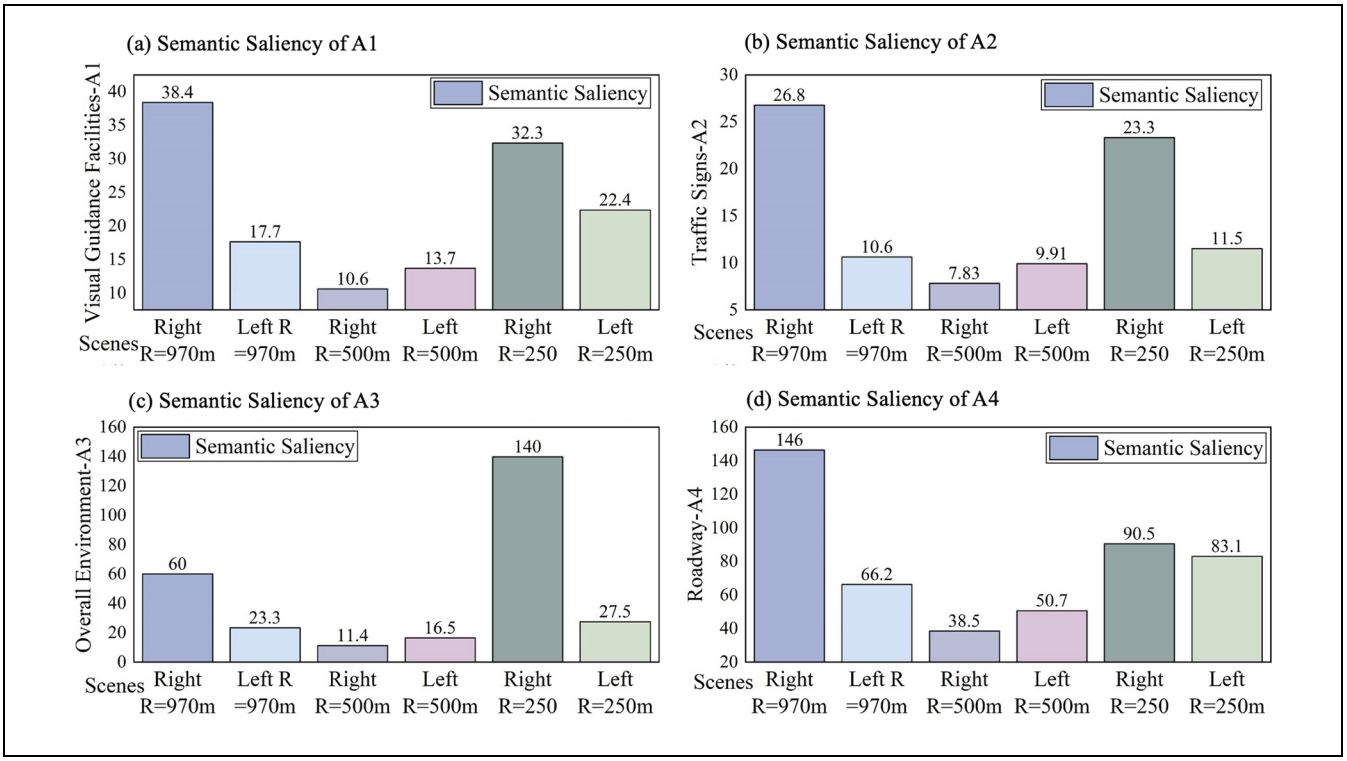

Figure 8. Calculation results of visually significance of four types of environmental element.

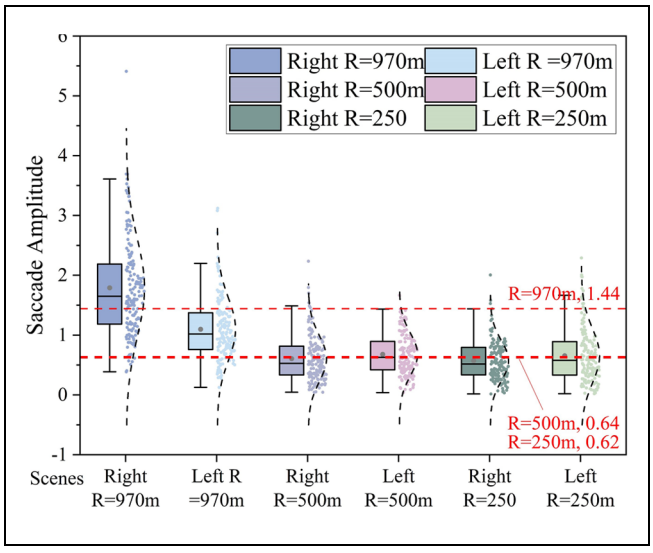

Figure 9. Calculation results of drivers' saccade amplitude.

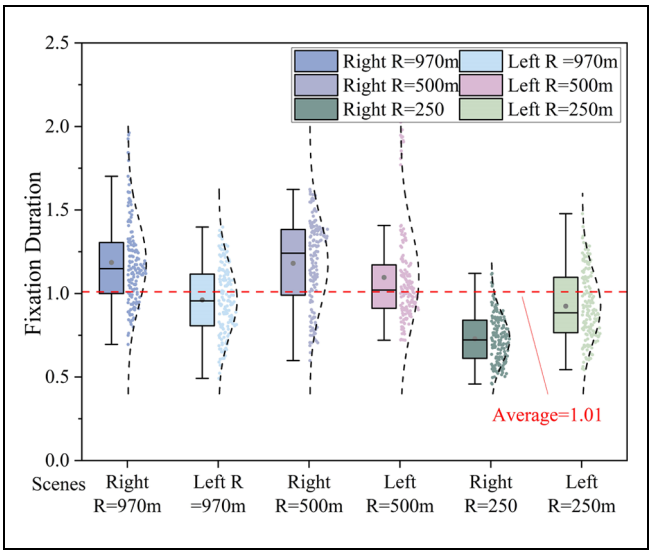

Figure 10. Calculation results of drivers' fixation duration.

below 30. The road body (A_4) (Figure 8 (*d*)), generally has the highest saliency values in all scenarios, with right turn R = 970 m at 146.31, followed by right turn R = 250 m (90.52), and left turn R = 250 m and left turn R = 970 m at 83.05 and 66.23, respectively. The values for both turns at R = 500 m are relatively small (38.53 and 50.65). These results suggest that the saliency of environmental elements is jointly influenced by curve radius and turn direction. Although the roadway layout was kept consistent across scenarios, differences in visual occlusion and viewing angle may lead to substantial differences between left- and right-turn conditions.

Saccade Amplitude. As shown in Figure 9, the overall distribution of drivers' saccade amplitudes under six spiral tunnel conditions is approximately between 0 and 3, with a small number of outliers that can approach 5. Looking at the overall level for different radius, the average saccade amplitudes given by the red dashed line in the figure are as follows: the average value is 1.60 for R = 970 m, which is higher than the average of about 0.72 for R = 500 m and the average of about 0.66 for R = 250 m. Observing by scenario, the box height is the highest for the right turn scenario at R = 970 m, with a median of about 1.5 to 2.0, and the interquartile range and scatter range are also relatively large; the average value for the left-turn scenario at R = 970 m is lower, around 0.72. In the R = 500 m condition, the median values for both the right-turn and left-turn scenarios are in the range of about 0.6 to 0.8, and the box height is relatively small. Under the R = 250 m condition, the average value for the right-turn scenario is around 0.6, while the left-turn scenario is slightly higher, around 0.7 to 0.8, with the overall distribution concentrated below 1.5.

Results of Comprehensive Attribute of the Road

Fixation Duration. As shown in Figure 10, the overall distribution of drivers' fixation duration under the six spiral tunnel conditions is concentrated between 0.5 and 1.5, with a small number of outliers nearing 2. The average fixation duration summarized by turning and radius conditions is indicated by the red dashed line in the figure, with an average value of 1.01. Specifically, the median fixation duration in the right-turn R = 970 m scenario is approximately 1.4, significantly higher than that in the other conditions; the median in the left-turn R = 970 m scenario is slightly lower, at approximately 1.2. In the R = 500 m scenario, the medians for right and left turns are 1.0 and 0.9, respectively, with a relatively concentrated overall distribution. In the R = 250 m scenario, the median for right turns is close to 1.0, while that for left turns is slightly below 0.9. The overall fixation duration is the shortest among all conditions and is relatively compactly distributed.

LH/FH. As shown in Figure 11, the average LH/FH values of drivers under six spiral tunnel conditions range from 1.03 to 3.34. Specifically, for the right turn with a radius of R = 970 m, the LH/FH is 1.45, while for the left turn with the same radius, it is 1.06; for the right turn with a radius of R = 500 m, LH/FH is 1.03, and for the left turn with the same radius, it is 1.32; for the right turn with a radius of R = 250 m, LH/FH is 1.95, and for the left turn with the same radius, it is 3.34. After

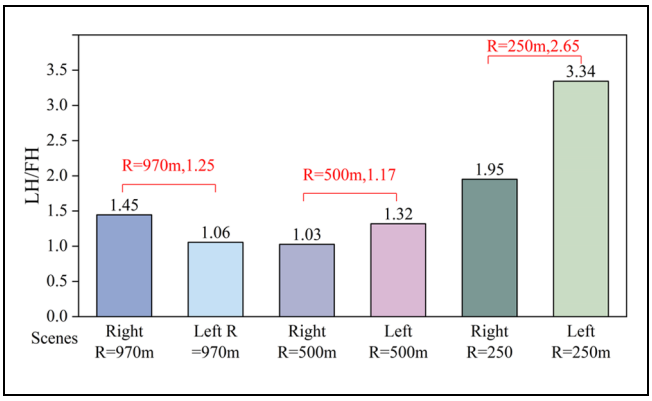

Figure 11. Calculation results of driver's LH/FH (Low-Frequency / High-Frequency).

summarizing by curvature, the average LH/FH under three radius conditions is indicated in red in the figure: the average value is 1.25 for R = 970 m, 1.17 for R = 500 m, and 2.65 for R = 250 m. Overall, drivers exhibit the highest cognitive effort under small-radius spiral conditions, especially in the left-turn scenario.

Results of Behavioral Indicators

Acceleration and Speed. As shown in Figure 12, the acceleration changes under six different turning and radius conditions exhibit different trends. For the right turn with R = 970 m (Figure 12*a*) and the left turn with R = 970 m (Figure 12*d*), the acceleration shows a downward trend as the spiral angle increases. However, for the right turn with R = 500 m (Figure 12*b*) and the left turn with R = 500 m (Figure 12*e*), the acceleration first increases and then decreases, presenting a relatively smooth curve. The acceleration curves for the right turn with R = 250 m (Figure 12*c*) and the left turn with R = 250 m (Figure 12*f*) fluctuate significantly, especially for the right turn with R = 250 m, where the acceleration fluctuates strongly in the smaller-angle sections.

As shown in Figure 13, the speed profiles under different turning directions and radii exhibited broadly consistent trends: drivers generally began to accelerate gradually after entering the tunnel, then decelerated for a certain distance before the exit, followed by a marked acceleration. Further focusing on the speed results within the spiral tunnel section (Figure 14), the speed changes at the entrance were generally small across all conditions, indicating that drivers mainly performed mild speed adjustments during the initial stage of entering the spiral tunnel. At the exit, however, the speed curves commonly showed larger fluctuations, suggesting that this region induced more substantial acceleration and deceleration behaviors. Combined with the average speed (v_{ave}) results, it can be observed that the overall speed level

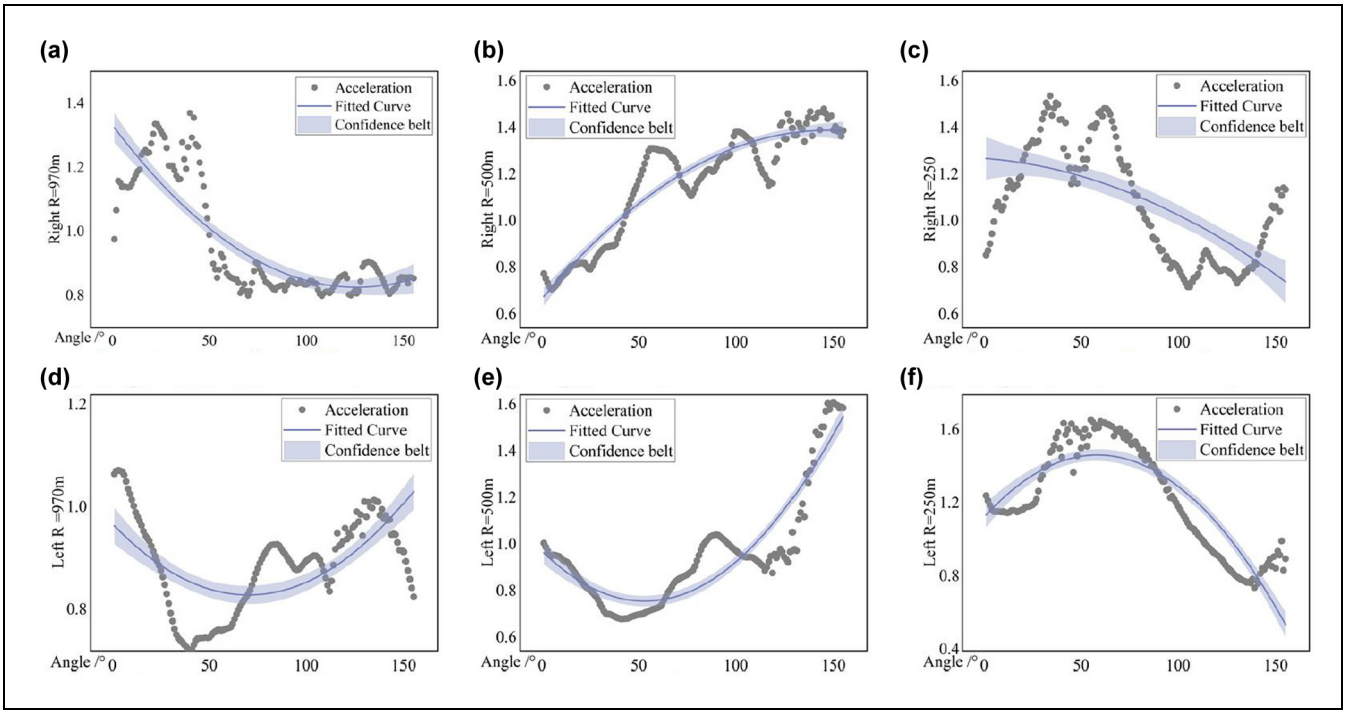

Figure 12. Calculation results of drivers' acceleration: (*a*) right turn, 970 m, (*b*) right turn, 500 m, (*c*) right turn, 250 m, (*d*) left turn, 970 m, (e) left turn, 500 m, and (*f*) left turn, 250 m.

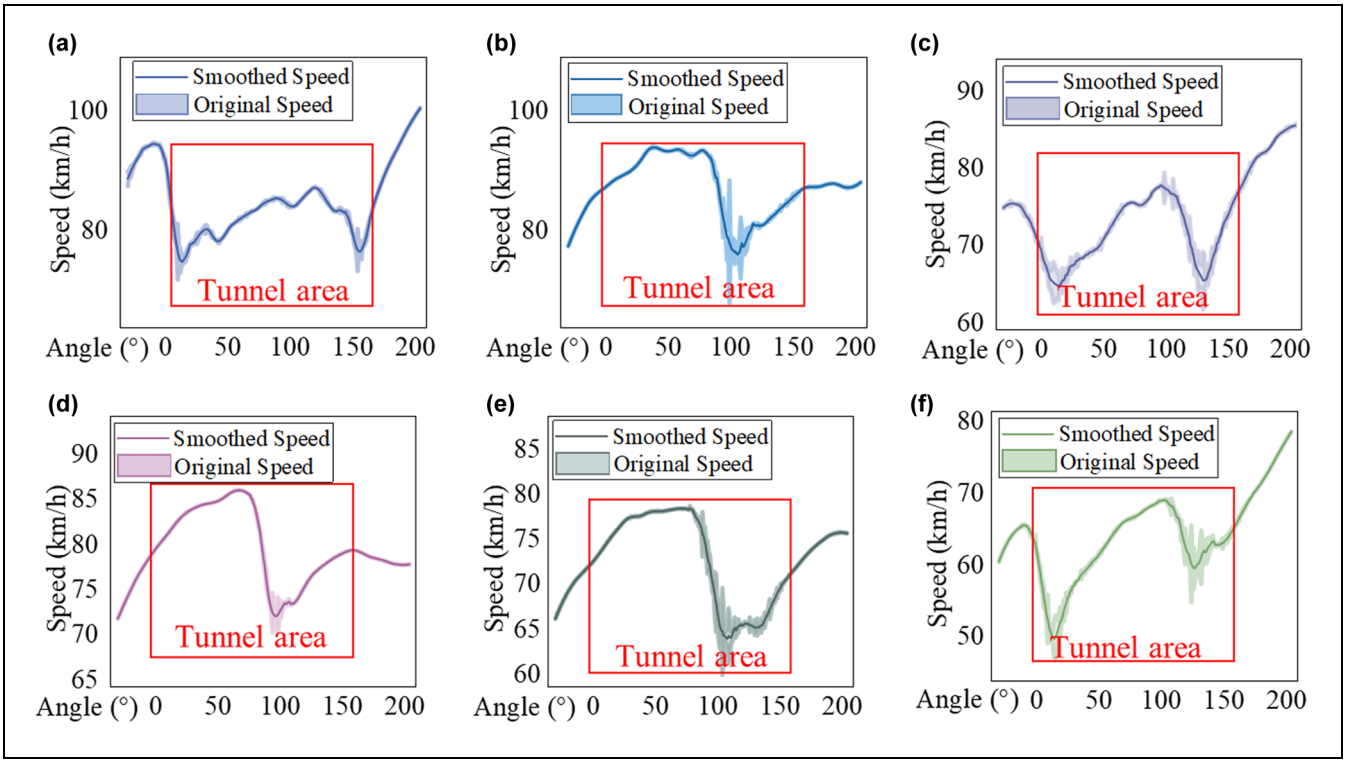

Figure 13. Vehicle speed profiles along the full road segment under different conditions (*a*) right turn, 970 m, (*b*) right turn, 500 m, (*c*) right turn, 250 m, (*d*) left turn, 970 m, (e) left turn, 500 m, and (*f*) left turn, 250 m.

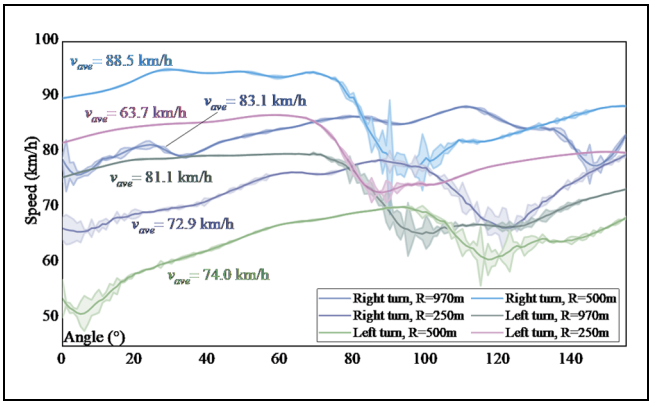

Figure 14. Comparison of vehicle speeds within the spiral tunnel section.

under right-turn conditions was higher than that under left-turn conditions, indicating that drivers maintained relatively higher operating speeds in right-turn spiral tunnels.

Trajectory Deviation. Based on the results in Figure 15, the trajectory deviation trends of drivers under six different turning and radius conditions vary. Overall, the trajectory deviations for right turns R = 970 m and left turns R = 970 m are relatively small and exhibit smooth fluctuations, especially within the first 50°. Right turns R = 500 m and left turns R = 500 m show some fluctuations, particularly within the range of 90° to 130° of the turning angle, where the deviation changes significantly. Right turns R = 250 m and left turns R = 250 m exhibit strong fluctuations, with larger deviation values, especially within the range of 100° to 140°, where the deviation increases significantly. Overall, the trajectory deviations are smaller and the fluctuations are smoother in scenarios with larger radii, while the deviations fluctuate more in scenarios with smaller radii. Additionally, right-turn conditions generally show greater trajectory deviations, indicating that drivers' trajectories are more unstable under small radius conditions.

Self-Explaining Level

The calculation results are presented in Table 3. Spiral tunnels with different turning directions exhibit significant differences in perceptual attributes, comprehension attributes, and overall self-explaining level. Left-turn spiral tunnels show generally lower perceptual attributes ($f^* = 117.7$), with lower comprehension attribute values ($V = 0.791$) and a lower self-explaining level ($S = 19.0$) than right-turn tunnels.

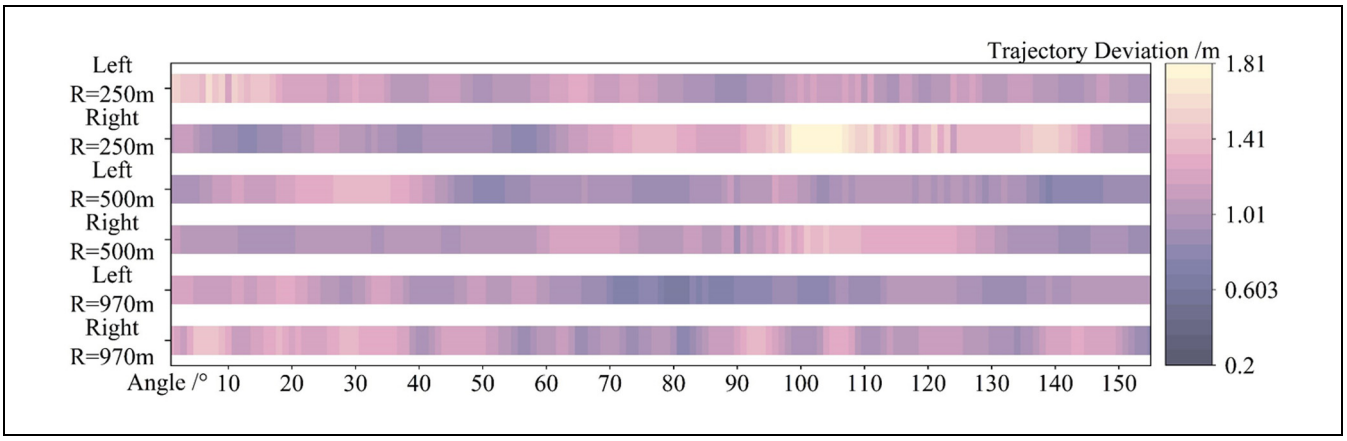

Figure 15. Calculation results of drivers' trajectory deviation.

Table 3. Self-Explaining Levels with Different Turning Directions

Turning direction	f_j				f^*	V/s^{-1}	S
	f_1	f_2	f_3	f_4			
Right	19.4	13.8	27.9	75.1	136.3	0.876	20.0
Left	17.9	10.7	22.4	66.6	117.7	0.791	19.0

Table 4. Self-Explaining Levels with Different Radius

Radius (m)	f_j				f^*	V/s^{-1}	S
	f_1	f_2	f_3	f_4			
$R = 250$	15.8	9.2	20.0	61.7	106.8	0.777	9.9
$R = 500$	12.2	8.9	13.9	44.6	79.5	0.900	21.0
$R = 970$	28.0	18.7	41.6	106.3	194.6	0.824	27.6

The calculation results are presented in Table 4. The self-explaining level of spiral tunnels increases as the curve radius increases: when the radius is 250 m, $S = 9.9$; it rises to 21.0 at 500 m, and further increases to 27.6 at the maximum radius of 970 m. This trend indicates that spiral tunnels with higher radii are more effective at triggering drivers' perception, comprehension, and projection processes, thereby achieving a higher level of self-explanation.

As shown in Figure 16, both right-turn and left-turn spiral tunnels exhibit a dynamic variation in self-explaining level with respect to turning angle, generally following a pattern of "initial decline—subsequent rise—fluctuation—final drop." Before entering the tunnel, the self-explaining level decreases, reflecting increased uncertainty in driver expectations caused by the unfamiliar environment ahead. After entering the tunnel, as drivers begin to adapt to the scene, the level increases and tends to stabilize in the middle segment. Near the exit, the self-explaining level fluctuates again, influenced by changes in lighting and tunnel structure, before declining at the end.

Discussion

Drivers' Visual and Cognitive Characteristics within Spiral Tunnels

According to the calculation results of the semantic saliency of different environments (Figure 8), this study found that the saliency value of roadway region (A_4) was generally the highest across all scenes. Specifically, in the

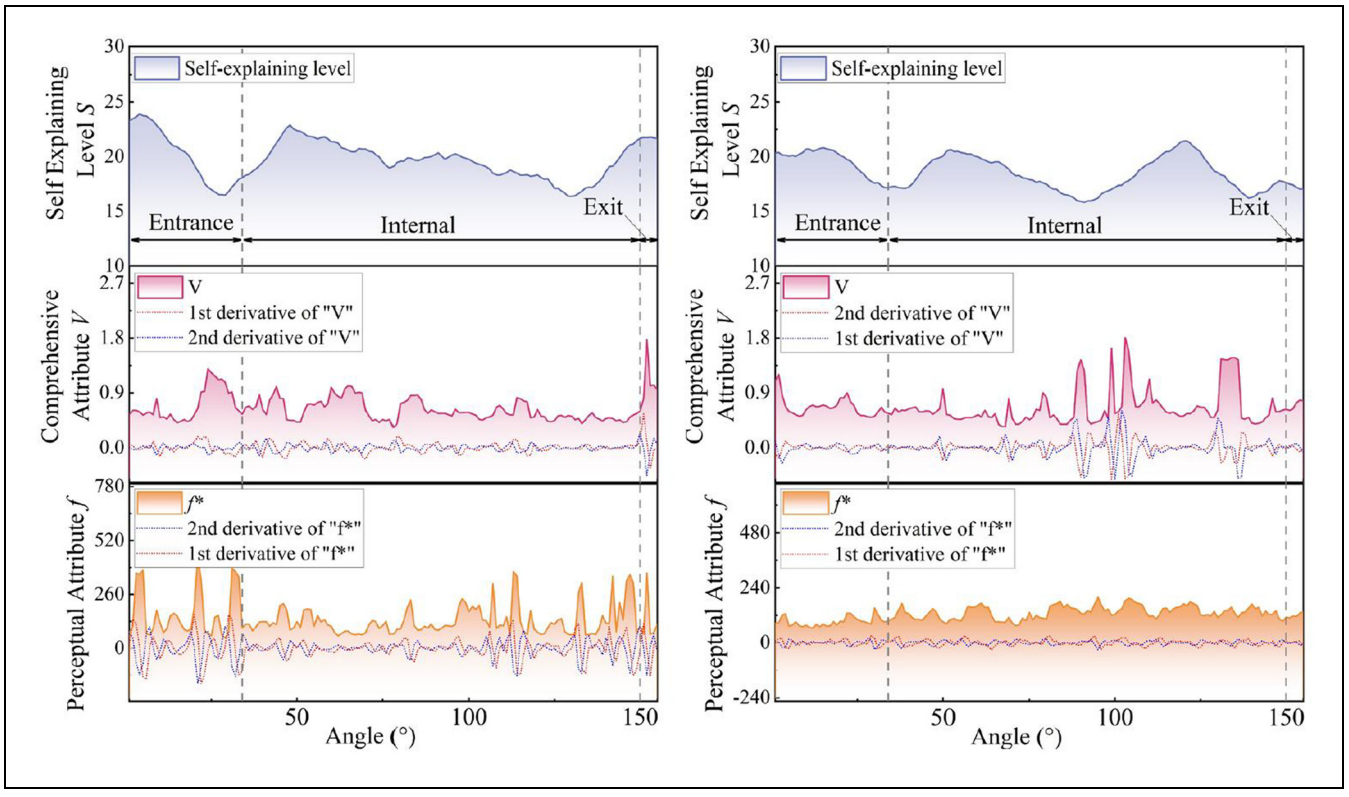

Figure 16. Variation of self-explaining level with spiral turning angle: right-turn scenario (*left*) and left-turn scenario (*right*).

right-turn R = 970 m scenario, the saliency reached 146.31, which was significantly higher than under other conditions. This indicates that the visual saliency of roadway region plays a key role in improving the self-explaining level. Moreover, the successful integration of environmental semantic segmentation into the proposed framework enables a clearer identification of the contribution of different facility semantics to driver cognition at the theoretical level, while also providing parameter-level support for facility optimization in practical tunnel design. In contrast, in a small-radius scenario (e.g., R = 250 m), the roadway region is less salient, which may be because of the occlusion of the driver's sight at smaller curve radii, increasing the difficulty of obtaining visual information. Additionally, the significance of visual guidance facilities in the right-turn R = 250 m and left-turn R = 250 m scenarios is lower, likely because of the smaller visual field and increased visual interference (*41*).

The substantial left–right difference observed may be explained by direction-dependent visual exposure. In the right-turn scenario, some facilities and roadway elements are likely to enter the driver's field of view earlier, making them more readily perceived and thus yielding higher semantic saliency. By contrast, in the left-turn scenario, stronger occlusion from the inner tunnel wall may limit the effective visual range, thereby weakening the perceptual saliency of the environmental elements. From a theoretical perspective, the integration of environmental semantic segmentation provides data-level support for investigating driver visual perception by enabling the quantification of the saliency contribution of different environmental semantics. From a practical perspective, the results suggest that, in left-turn scenarios, the saliency of environmental facilities should be enhanced through design measures such as larger facility dimensions or denser spacing arrangements.

Visual search is the primary means for drivers to obtain environmental information (*42*). Under different tunnel conditions with varying radii, there are significant differences in the saccade amplitude of drivers (Figure 9): the average saccade amplitude in the R = 970 m scenario is 1.60, which is higher than that in the R = 500 m (0.72) and R = 250 m (0.66) scenarios. In this study, saccade amplitude was used to characterize visual search span during the perception stage. A larger saccade amplitude in the large-radius tunnels may reflect a broader visual field and more flexible information sampling. As shown in Figure 10, fixation duration did not exhibit the same trend as LH/FH across all scenarios. Although it was generally shorter in the R = 250 m condition, the LH/

FH ratio in Figure 11 was the highest, especially in the left-turn scenario, indicating increased cognitive effort during information processing. This suggests that that small-radius spiral tunnels impose greater overall cognitive demands on drivers, whereas large-radius tunnels provide a wider visual field and more stable information-processing conditions, thereby supporting a higher self-explaining level.

Underwood et al. found that fixation duration is influenced by driving load, implying that higher driving loads lead to longer extraction and processing times of road traffic information (*43*). When the information stimulus intensity is insufficient, visual load decreases accordingly (*44*). This suggests that in tunnels with larger radius, drivers exhibit larger saccade amplitudes, possibly because the wider field of view allows drivers to obtain more environmental information, thereby reducing cognitive tension. Consistent with the findings of Han et al., drivers in left-turn tunnels tend to exhibit longer fixation durations, lower fixation frequency, shorter saccade times, and larger saccade amplitudes (*20*, *21*). Overall, left-turn spiral tunnels may lead to cognitive consequences such as overlooking or misinterpreting certain environmental information, resulting in a lower level of self-explanation. Therefore, when designing tunnels with smaller radius, consideration can be given to extending the drivers' fixation time and providing more time for information processing by adjusting the lighting, signs, and visual guidance equipment within the tunnel to reduce visual fatigue and cognitive effort. However, it should be noted that these conclusions only represent a general trend, and lack precision. To more comprehensively explore the complex relationship between fixation behavior and cognitive load in spiral tunnels, future research should employ more advanced experiment equipment.

Relationship between Self-Explaining Level and Drivers' Behaviors

Based on the existing conditional probability model of situational awareness, this paper integrates the salience of environmental semantic information at the perception end and establishes a model with self-explaining levels. Through Spearman's rank correlation analysis in this study, it was found that there is a significant correlation between self-explaining level and driving behavior indicators (e.g., acceleration and trajectory deviation) in most tunnel scenarios. Especially in tunnels with larger curvature (R = 970 m) and smaller curvature (R = 250 m), a negative correlation was observed between the two (correlation coefficients ranging from -0.234 to -0.326, with p-values all less than 0.001). This result indicates that the higher the self-explaining level, the smoother the drivers' operation and the smaller the fluctuations.

The acceleration of drivers in spiral tunnels varies with the change in driving angle, following a certain pattern (Figure 12). Under conditions of medium and small radius, drivers' acceleration near the tunnel exit shows a noticeable upward trend, indicating significant speed fluctuations and poor stability at the exit. In the special structure of spiral tunnels, continuous and uniform driving may induce drivers to develop a driving inertia. When approaching the tunnel exit, the strong "white hole effect" may lead drivers to misjudge the radius (overestimating the radius size), thereby tending to alter their previously stable driving state (*10*). This result is consistent with previous field-based research on spiral tunnels, which reported that the tunnel exit is a critical zone where abrupt illumination changes and altered driving expectations significantly disturb speed control and increase driving risk (*45*). Therefore, because of the multiple influences of risk perception and visual illusion, the correlation between drivers' acceleration changes and self-explaining levels is weaker than trajectory deviation. Therefore, we recommend enhancing the environmental design at the exit of spiral tunnels and installing prominent visual navigation facilities to improve drivers' correct perception of the geometry of spiral tunnels.

The lane-keeping performance of drivers in spiral tunnels is influenced by the self-explaining performance of lateral facilities in the tunnel environment, reflecting the accuracy of drivers' perception of lateral position (*7*). The deviation of vehicle trajectory is a direct measure of lane keeping performance (*46*, *47*). Behavioral data analysis (Figure 13) indicates that right turns and geometric features with small radius tend to have larger and more unstable trajectory deviations. A literature review reveals that this phenomenon may be related to the side wall effect of tunnels (*42*). In this study, the simulation adopted a left-side driving configuration and drivers were guided to drive in the right lane, which means they were closer to the side wall when making right turns, thus tending to move away from the side wall (the average trajectory deviation during right turns was 1.15 m, compared with 1.04 m during left turns). Furthermore, behavioral data analysis (Figures 12 and 13) shows that in tunnels with larger radius, acceleration changes are smoother and trajectory deviations are smaller, whereas in tunnels with smaller radius, there are greater fluctuations in acceleration and trajectory deviations. This is consistent with the calculation results of self-explaining level, indicating that spiral tunnels with larger radius have higher scores. Therefore, we recommend enhancing the lateral clearance on the same side of the lane as the turning direction for tunnels with smaller radius to alleviate the side wall effect on drivers, thereby reducing visual obstruction from the wall (*48*). Future studies may

further collect floating car data data to analyze real-world vehicle trajectories (*49*).

Relationship between Self-Explaining Level and Geometric Features of Spiral Tunnels

The results in Table 2 indicate that left-turn spiral tunnels face more unfavorable conditions in driving perception and comprehension, exhibiting a lower level of self-explanation. One possible reason is that, because of visual obstruction caused by the tunnel wall on the inner side of the curve, the perceptual attribute of the road body in left-turn tunnels is the lowest ($f_4 = 66.6$), and other types of environmental information are also more difficult to perceive than in right-turn conditions. Turning left in the left lane is commonly regarded as an unfavorable condition. Another possible reason is that most participants were right-handed, but this requires further experiment verification. This type of road environment, which is difficult for drivers to perceive, may lead to continuous scanning of the surroundings to extract more useful information from the environment (resulting in longer saccade distances and more dispersed fixation points). The lower comprehension attribute observed under left-turn conditions indicates that drivers must consume more attentional resources to interpret road information, as reflected by the combined pattern of physiological activation and visual processing demand.

From the perspective of different radius, the overall perception attribute value is relatively high at a radius of 970 m ($f^* = 194.6$), which may be because of the wider field of view provided by curves with larger radius (Figure 14 shows that the saliency of road information at a right turn of 970 m, A4 = 160, is much higher than in other scenarios). Interestingly, although the perception attribute of the spiral tunnel with a radius of 250 m ($f^* = 106.8$) is higher than that of the tunnel with a radius of 500 m ($f^* = 79.5$), this indicates that road information is more easily perceived by drivers. However, the comprehension attribute is lowest at a radius of 250 m ($V = 0.777$), suggesting that, although drivers can efficiently collect environmental information, they face challenges in processing it. Small-radius tunnels demand greater attentional resources, characterized by longer fixation durations and more cognitively demanding tasks, which aligns with the conclusions of Han et al. (*20*). This may result in slower responses and a higher likelihood of misinterpretation at the behavioral level. Supporting this, the behavioral data show that the 250 m radius tunnel has the larger acceleration ($1.10\,m/s^{-2}$, compared with $1.12\,m/s^{-2}$ for a radius of 500 m and $0.87\,m/s^{-2}$ for a radius of 970 m) and largest lateral position deviation (0.97 m, compared with 0.91 m for a radius of 500 m and 0.92 m for a radius of 970 m). The poorer performance observed in smaller-radius tunnels may also be attributed not only to lower environmental self-explanation, but also to the increased steering sensitivity and reduced sight distance inherently associated with tighter curves. To mitigate this issue, speed control can be implemented to allow drivers more time for information processing (*50*). Reduced driving speed grants driver additional cognitive bandwidth for interpreting the environment, especially on curvatures (*51*). Alternatively, driver training focused on navigating small-radius tunnels could help drivers develop mental representations or schemas of such scenarios, enhancing their cognitive processing efficiency when encountering similar environments in the future.

Taking into account the traveling angle of a spiral tunnel, the locations of the entrances and exits exhibit significant fluctuations in driver perception and understanding. In particular, left-turn tunnels exhibit smaller fluctuations in perceptual attributes, indicating relatively stable visual input. However, the comprehension attribute shows more intense variability, suggesting greater cognitive adjustment or difficulty in processing environmental changes. These findings highlight the importance of considering spatial position and turning direction when designing tunnel environments, especially in transitional zones such as entrances and exits. Enhancing visual guidance and reducing environmental uncertainty in these areas could significantly improve the road's self-explaining effectiveness and overall driving safety.

Conclusion

This study addresses the issues of high cognitive load and elevated operational risk in spiral tunnels by developing a quantitative model of self-explaining level based on the SER theory. Integrating environmental semantic segmentation and the three-level situational awareness model, the study proposes perceptual and comprehension attribute indicators, and validates the model through driving simulation experiments. The results demonstrate that the model effectively captures how road environments guide driver cognition. Key findings include:

1) The self-explaining level is significantly correlated with driving behavior. The study found a statistically significant negative correlation between self-explaining level and driving performance indicators, such as acceleration and trajectory deviation, particularly in spiral tunnels with large (R = 970 m) and small (R = 250 m) radii. For example, in the right-turn R = 970 m and right-turn R = 250 m scenarios, the correlation coefficients ranged from -0.234 to -0.326 ($p < 0.001$), indicating smoother driving behavior as the self-explaining level increases.

2) Road region semantics showed the highest saliency across all scenarios, with the maximum value observed in the right-turn R = 970 m condition (146.31). Environmental semantic saliency shows clear left–right differences, and semantic segmentation enables a parameterized interpretation of such differences. In particular, under the right-turn condition, the saliency of visual guidance facilities, traffic signs, and roadway region was consistently higher than in the left-turn condition, indicating substantial direction-dependent perceptual asymmetry. By integrating environmental semantic segmentation, the study further quantified the saliency contribution of different facility semantics, providing parameter-level support for perceptual analysis and facility optimization.
3) Right-turn spiral tunnels exhibit higher self-explaining levels than left-turn counterparts (20.0 versus 19.0), mainly because of richer spatial semantics and more effective cognitive processing. In particular, left-turn tunnels were associated with higher cognitive load, reflected in lower perceptual efficiency, elevated physiological demand, and less favorable overall comprehension performance.
4) Large-radius spiral tunnels correspond to stronger self-explaining capability. The study found that larger radius (R = 970 m) enhances the self-explaining level (27.6), as these tunnels provide a wider visual field for drivers, reducing cognitive tension and facilitating information processing. In contrast, small-radius tunnels (R = 250 m) impose higher cognitive demands, as evidenced by greater fluctuations in acceleration and trajectory deviation, and lower self-explaining levels (9.9).
5) Entrance and exit areas introduce cognitive fluctuations caused by abrupt changes in lighting and structure, highlighting the need for targeted optimization in these critical zones. For example, the self-explaining level decreases near tunnel entrances because of visual uncertainty, while fluctuations are observed near the exits, especially in smaller-radius tunnels, indicating that enhancing visual guidance and reducing environmental uncertainty in these areas could improve driver perception and safety.

Although this research establishes a quantifiable cognitive assessment framework, it remains primarily evaluative in nature and does not yet provide concrete environmental design solutions. Future work will expand the model's application in engineering practice, develop cognition-friendly tunnel design strategies, and conduct validation through simulation and real-vehicle testing. It should also be noted that the transition from open environments to enclosed tunnel spaces may involve visual adaptation effects because of rapid changes in illumination. Such physiological responses cannot be fully reproduced in driving simulators. Therefore, although the simulator provides a controlled environment for evaluating driver perception and behavior, the influence of real-world light adaptation at tunnel entrances may not be completely captured. Future studies could further validate the findings through field experiments or naturalistic driving data.

Author Contributions

The authors confirm contribution to the paper as follows: study conception and design: Y. Xia, C. Zhang; data collection: Y. Xia, Y. Gao; analysis and interpretation of results: B. Wang, X. Yan, Y. Xia; draft manuscript preparation: Y. Xia, B. Wang. All authors reviewed the results and approved the final version of the manuscript.

Declaration of Conflicting Interests

The authors declared no potential conflicts of interest with respect to the research, authorship, and/or publication of this article.

Funding

The authors disclosed receipt of the following financial support for the research, authorship, and/or publication of this article: This work was supported by the Fundamental Research Funds for the Central Universities (Grant No. CHD300102215206), the National Key Research & Development Program of China (Grant No. 2020YFC1512003), the Sichuan Science and Technology Program (Grant No. 2022YFG0048), the Science and Technology Project of Sichuan Transportation Department (Grant No. 2022-ZL-04), and the Key Research and Development Program of Shaanxi Province (Grant No. 202102020101014].

ORCID iDs

Yanzi Xia https://orcid.org/0009-0003-2197-172X
Chi Zhang https://orcid.org/0000-0003-0713-3722
Bo Wang https://orcid.org/0000-0002-0593-6612
Xiaomin Yan https://orcid.org/0009-0004-9996-6127
YanYang Gao https://orcid.org/0009-0001-5818-6106
Yijing Zhao https://orcid.org/0009-0004-7189-9217

Data Accessibility Statement

The data underlying this study are not publicly available because they are subject to informed-consent, privacy, and ethics restrictions.

References

1. Zhang, C., C. Wang, X. Niu, S. Zhang, and H. Zhao. Effect of the Double-Line Spiral Tunnel Curvature on the Tunnel Construction Stability. *Advances in Civil Engineering*, Vol. 2020, 2020, pp. 1–9. https://doi.org/10.1155/2020/8827806.
2. Jiang, Y., J. Yu, P. Zhou, F. Zhou, J. Lin, J. Li, M. Lin, F. Lei, and Z. Wang. Influence of Traffic on the Temperature Field of Tunnel in Cold Region: A Case Study on the World's Longest Highway Spiral Tunnel. *Underground Space*, Vol. 8, 2023, pp. 196–209. https://doi.org/10.1016/j.undsp.2022.03.002.
3. Du, Z., L. Han, J. Mei, S. He, and Y. Yang. Visual Environment Optimization Framework for Long Highway Tunnels with Small Radii Based on Mental Rotation Effect. *Journal of Tongji University (Natural Science)*, 2023. 51(9):1372–1382.
4. Han, L., Z. Du, and S. Wang. The Impact of Spiral Tunnel Characteristics on Driver HRV and Stress Perception: A Naturalistic Driving Experiment. *Accident Analysis & Prevention*, Vol. 214, 2025, p. 107983. https://doi.org/10.1016/j.aap.2025.107983.
5. Wan, H., Y. Jiang, and J. Jiang. A Survey of Fire Accidents during the Process of Highway Tunnel Operation in China from 2010 to 2021: Characteristics and Countermeasures. *Tunnelling and Underground Space Technology*, Vol. 139, 2023, p. 105237. https://doi.org/10.1016/j.tust.2023.105237.
6. Theeuwes, J., and H. Godthelp. Self-Explaining Roads. *Safety Science*, Vol. 19, No. 2–3, 1995, pp. 217–225. https://doi.org/10.1016/0925-7535(94)00022-U.
7. Xing, G., Y. Ma, S. Chen, Y. Xing, Q. Pang, and L. Gao. Investigating the Self-Explaining Performance of Visual Guidance Facilities in Extra-Long Spiral Tunnels Based on Drivers' Spatial Perception and Visual Attention Distribution. *Accident Analysis & Prevention*, Vol. 217, 2025, p. 108040. https://doi.org/10.1016/j.aap.2025.108040.
8. Jiao, F., Z. Du, Y. D. Wong, S. He, F. Xu, and H. Zheng. Self-Explaining Performance of Visual Guiding Facilities in Urban Road Tunnels Based on Speed Perception. *Tunnelling and Underground Space Technology*, Vol. 122, 2022, p. 104371. https://doi.org/10.1016/j.tust.2022.104371.
9. Yan, Y., Y. Zhang, H. Yuan, L. Wan, and H. Ding. Safety Effect of Tunnel Environment Self-Explaining Design Based on Situation Awareness. *Tunnelling and Underground Space Technology*, Vol. 143, 2024, p. 105486. https://doi.org/10.1016/j.tust.2023.105486.
10. Xia, Y., C. Zhang, M. Zhang, H. Zhang, and B. Wang. Characterizing the Driving Cognition within Spiral Tunnels Based on SER Principle. *Tunnelling and Underground Space Technology*, Vol. 163, 2025, p. 106649. https://doi.org/10.1016/j.tust.2025.106649.
11. Endsley, M. R. A Systematic Review and Meta-Analysis of Direct Objective Measures of Situation Awareness: A Comparison of SAGAT and SPAM. *Human Factors*, Vol. 63, No. 1, 2021, pp. 124–150. https://doi.org/10.1177/0018720819875376.
12. Theeuwes, J., J. Snell, T. Koning, and B. Bucker. Self-Explaining Roads: Effects of Road Design on Speed Choice. *Transportation Research Part F: Traffic Psychology and Behaviour*, Vol. 102, 2024, pp. 335–361. https://doi.org/10.1016/j.trf.2024.03.007.
13. Xia, Y., C. Zhang, M. Zhang, H. Zhang, and B. Wang. Characterizing the Driving Cognition within Spiral Tunnels Based on SER Principle. *Tunnelling and Underground Space Technology*, Vol. 163, 2025, p. 106649. https://doi.org/10.1016/j.tust.2025.106649.
14. Li, M., Z. Feng, W. Zhang, L. Wang, L. Wei, and C. Wang. How Much Situation Awareness Does the Driver Have When Driving Autonomously? A Study Based on Driver Attention Allocation. *Transportation Research Part C: Emerging Technologies*, Vol. 156, 2023, p. 104324. https://doi.org/10.1016/j.trc.2023.104324.
15. Steelman, K. S., J. S. McCarley, and C. D. Wickens. Theory-Based Models of Attention in Visual Workspaces. *International Journal of Human–Computer Interaction*, Vol. 33, No. 1, 2017, pp. 35–43. https://doi.org/10.1080/10447318.2016.1232228.
16. Lindenberg, S.How Cues in the Environment Affect Normative Behaviour. In *Environmental Psychology* (L. Steg, and J. I. M. Groot, eds.), Hoboken, NJ, USA: Wiley, pp. 144–153. https://doi.org/10.1002/9781119241072.ch15.
17. Abdulrazaq, M. A., and W. (David) Fan. A Priority Based Multi-Level Heterogeneity Modelling Framework for Vulnerable Road Users. *Transportmetrica A: Transport Science*, Vol. 32, No. 3, pp. 499–522. https://doi.org/10.1080/23249935.2025.2516817.
18. Talebpour, A., Y. Zhang, T. Radvand, and M. Yousefi. *Advancing Self-Enforcing Streets Phase 1: The Relationship between Roadway Environment and Crash Severity*. Publication FHWA-ICT-24-023. University of Illinois Urbana-Champaign, Illinois Center for Transportation, Urbana, IL, 2024.
19. Ren, W., B. Yu, Y. Chen, K. Gao, S. Bao, Z. Wang, and Y. Qin. An Intelligent Optimization Method for the Facility Environment on Rural Roads. *Computer-Aided Civil and Infrastructure Engineering*, Vol. 39, No. 17, 2024, pp. 2559–2580. https://doi.org/10.1111/mice.13209.
20. Han, L., Z. Du, and S. Wang. Assessment of Drivers' Visual Search Patterns and Cognitive Load During Driving in Curved Tunnels. *Traffic Injury Prevention*, Vol. 26, No. 5, 2025, pp. 524–534. https://doi.org/10.1080/15389588.2024.2441879.
21. Han, L., Z. Du, S. Wang, and S. He. The Effects of Tunnel Radius, Turn Direction, and Zone Characteristics on Drivers' Visual Performance. *Tunnelling and Underground Space Technology*, Vol. 152, 2024, p. 105912. https://doi.org/10.1016/j.tust.2024.105912.
22. Bei, R., Z. Du, T. Huang, J. Mei, S. He, and X. Zhang. Analysis and Regulation of Driving Behavior in the Entrance Zone of Freeway Tunnels: Implementation of Visual Guidance Systems in China. *Accident Analysis & Prevention*, Vol. 202, 2024, p. 107600. https://doi.org/10.1016/j.aap.2024.107600.
23. Zheng, H., Z. Du, C. Jia, L. Zhu, S. He, and J. Mei. Evaluating the Effectiveness of Rhythmic Visual Guidance Technology for Mitigating Driving Risks in Highway Tunnel Groups: A Simulation Study. *Accident Analysis &*

Prevention, Vol. 212, 2025, p. 107940. https://doi.org/10.1016/j.aap.2025.107940.
24. Shang, T., H. Lu, P. Wu, and X. Lu. Method of Setting Exit Advance Guide Signs in Highway Tunnels Based on the Driver's Eye Movement with Markov Chains. *IEEE Access*, Vol. 9, 2021, pp. 24079–24092. https://doi.org/10.1109/ACCESS.2021.3056090.
25. Shang, T., H. Lu, P. Wu, and Y. Wei. Eye-Tracking Evaluation of Exit Advance Guide Signs in Highway Tunnels in Familiar and Unfamiliar Drivers. *International Journal of Environmental Research and Public Health*, Vol. 18, No. 13, 2021, p. 6820. https://doi.org/10.3390/ijerph18136820.
26. Han, L., Z. Du, and A. Ma. Evaluation of Traffic Signs Information Volume at Highway Tunnel Entrance Zone Based on the Visual Sample Entropy of Novice and Experienced Drivers. *Traffic Injury Prevention*, Vol. 25, No. 3, 2024, pp. 499–509. https://doi.org/10.1080/15389588.2023.2300645.
27. Zeng, Q., Y. Chen, X. Zheng, S. He, D. Li, and B. Nie. Optimization of Underground Cavern Sign Group Layout Using Eye-Tracking Technology. *Sustainability*, Vol. 15, No. 16, 2023, p. 12604. https://doi.org/10.3390/su151612604.
28. He, S., B. Liang, G. Pan, F. Wang, and L. Cui. Influence of Dynamic Highway Tunnel Lighting Environment on Driving Safety Based on Eye Movement Parameters of the Driver. *Tunnelling and Underground Space Technology*, Vol. 67, 2017, pp. 52–60. https://doi.org/10.1016/j.tust.2017.04.020.
29. Kircher, K., and C. Ahlstrom. The Impact of Tunnel Design and Lighting on the Performance of Attentive and Visually Distracted Drivers. *Accident Analysis & Prevention*, Vol. 47, 2012, pp. 153–161. https://doi.org/10.1016/j.aap.2012.01.019.
30. Walker, G. H., N. A. Stanton, and I. Chowdhury. Self Explaining Roads and Situation Awareness. *Safety Science*, Vol. 56, 2013, pp. 18–28. https://doi.org/10.1016/j.ssci.2012.06.018.
31. Acerbi, L., W. J. Ma, and S. Vijayakumar. A Framework for Testing Identifiability of Bayesian Models of Perception. *Proceedings of the 28th International Conference on Neural Information Processing Systems*, Vol. 1, 2014, pp. 1026–1034. Cambridge, MA, USA: MIT Press. https://api.semanticscholar.org/CorpusID:1421438.
32. Theeuwes, J. Self-Explaining Roads: What Does Visual Cognition Tell Us about Designing Safer Roads? *Cognitive Research: Principles and Implications*, Vol. 6, No. 1, 2021, p. 15. https://doi.org/10.1186/s41235-021-00281-6.
33. Cheng, B., I. Misra, A. G. Schwing, A. Kirillov, and R. Girdhar. Masked-attention Mask Transformer for Universal Image Segmentation. *2022 IEEE/CVF Conference on Computer Vision and Pattern Recognition (CVPR)*, 2022, pp. 1280–1289. https://doi.org/10.1109/CVPR52688.2022.00135.
34. Min, J., Y. Zhao, C. Luo, and M. Cho. Peripheral Vision Transformer. *arXiv preprint arXiv:2206.06801*, 2022.
35. MMSegmentation Contributors. OpenMMLab Semantic Segmentation Toolbox and Benchmark. July, 2020. https://github.com/open-mmlab/mmsegmentation.
36. Wickens, C. D.Noticing Events in the Visual Workplace: The SEEV and NSEEV Models. In: *The Cambridge Handbook of Applied Perception Research. Cambridge Handbooks in Psychology* (R. R. Hoffman, P. A. Hancock, M. W. Scerbo, R. Parasuraman, and J. L. Szalma, eds.), Cambridge University Press; 2015, pp. 749–768.
37. Greaves, H. Epistemic Decision Theory. *Mind*, Vol. 122, No. 488, 2013, pp. 915–952. https://doi.org/10.1093/mind/fzt090.
38. Yang, Y., Y. Chen, S. M. Easa, J. Lin, M. Chen, and X. Zheng. Evaluation of Driver's Situation Awareness in Freeway Exit Using Backpropagation Neural Network. *Transportation Research Part F: Traffic Psychology and Behaviour*, Vol. 105, 2024, pp. 42–57. https://doi.org/10.1016/j.trf.2024.06.018.
39. Du, Z., S. Wang, L. Yang, and F. Jiao. Experimental Study on the Efficacy of Retroreflective Rings in the Curved Freeways Tunnels. *Tunnelling and Underground Space Technology*, Vol. 110, 2021, p. 103813. https://doi.org/10.1016/j.tust.2021.103813.
40. Xinhua News Agency. Ministry of Public Security Releases 2021 National Motor Vehicle and Driver Data. *Ministry of Public Security Releases 2021 National Motor Vehicle and Driver Data*. https://www.gov.cn/xinwen/2022-01/11/content_5667669.htm. Accessed November 26, 2024.
41. Han, L., P. Gu, H. Zhou, and Z. Du. Differential Blink Patterns as Biomarkers: Quantifying Visual Cognitive Load in Curved Tunnels with Varied Radii. *Traffic Injury Prevention*, pp. 1–10. https://doi.org/10.1080/15389588.2025.2569720.
42. He, S., Z. Du, L. Han, S. Wang, and Y. Chen. Impact of Urban Tunnel Sidewall Effect on Drivers: Examining Visual Characteristics and Driving Behavior across Different Lanes. *Tunnelling and Underground Space Technology*, Vol. 143, 2024, p. 105476. https://doi.org/10.1016/j.tust.2023.105476.
43. Underwood, G., D. Crundall, and P. Chapman. Driving Simulator Validation with Hazard Perception. *Transportation Research Part F: Traffic Psychology and Behaviour*, Vol. 14, No. 6, 2011, pp. 435–446. https://doi.org/10.1016/j.trf.2011.04.008.
44. Szychowska, M., and S. Wiens. Visual Load Effects on the Auditory Steady-State Responses to 20-, 40-, and 80-Hz Amplitude-Modulated Tones. *Physiology & Behavior*, Vol. 228, 2021, p. 113240. https://doi.org/10.1016/j.physbeh.2020.113240.
45. Xu, X., X. Kang, X. Wang, S. Zhao, and C. Si. Research on Spiral Tunnel Exit Speed Prediction Model Based on Driver Characteristics. *Sustainability*, Vol. 14, No. 23, 2022, p. 15736. https://doi.org/10.3390/su142315736.
46. Hu, H., Q. Wang, M. Cheng, and Z. Gao. Cost-Sensitive Semi-Supervised Deep Learning to Assess Driving Risk by Application of Naturalistic Vehicle Trajectories. *Expert Systems with Applications*, Vol. 178, 2021, p. 115041. https://doi.org/10.1016/j.eswa.2021.115041.
47. Shao, X., F. Chen, X. Ma, and X. Pan. The Impact of Lighting and Longitudinal Slope on Driver Behaviour in Underwater Tunnels: A Simulator Study. *Tunnelling and Underground Space Technology*, Vol. 122, 2022, p. 104367. https://doi.org/10.1016/j.tust.2022.104367.
48. Chen, Y., Z. Du, J. Xu, and S. Luo. Driving Characteristics of Static Obstacle Avoidance by Drivers in Mountain Highway Tunnels − A Lateral Safety Distance Judgement.

Accident Analysis & Prevention, Vol. 210, 2025, p. 107845. https://doi.org/10.1016/j.aap.2024.107845.

49. Zhang, C., Y. Zhou, M. Zhang, B. Wang, and Y. Nie. Review and Prospect of Floating Car Data Research in Transportation. *Journal of Traffic and Transportation Engineering (English Edition)*, Vol. 12, No. 4, 2025, pp. 752–771. https://doi.org/10.1016/j.jtte.2024.09.005.
50. Köhler, A.-L., M. Klatt, I. Koch, and S. Ladwig. Investigating the Influence of Visuospatial Stimuli on Driver's Speed Perception: A Laboratory Study. *Cognitive Research: Principles and Implications*, Vol. 8, No. 1, 2023, p. 59. https://doi.org/10.1186/s41235-023-00513-x.
51. Abdulrazaq, M. A., and W. D. Fan. Temporal Dynamics of Pedestrian Injury Severity: A Seasonally Constrained Random Parameters Approach. *International Journal of Transportation Science and Technology*, 2024. https://doi.org/10.1016/j.ijtst.2024.11.009.